

Fig. 2. (a) Illustration of the edge currents on a bow-tie slot antenna. (b) Illustration of the longer edge currents on the compact bow-tie slot antenna.

The first method involves a modification of the radiating slots in the bow-tie slot antenna. Initially, the diagonal straight edges of the bow-tie slot antenna are redesigned to resemble a parametric curve. This parametric curved surface starts from the CPW transmission line feeding the antenna in Fig. 1 and ends with small circles subtracted from the points of the radiating slot. The combination of the parametric curved surfaces and circles forces currents traveling along the edge of the slot into a longer path. The second method involves extending the CPW transmission line feeding the antenna farther into the ground plane. Extending two narrow slits, mirroring the CPW configuration, to the upper half of the antenna forces a majority of the current from the feed into a longer path. A pictorial representation of the current flow on a bow-tie slot antenna and a compact bow-tie slot antenna is shown in Fig. 2(a) and (b), respectively.

For the following discussion and presentation of results, the lower and upper resonant frequencies are denoted as  $f_1$  and  $f_2$ , respectively. Similarly, the wavelengths of the lower and upper resonant frequencies are denoted as  $\lambda_1$  and  $\lambda_2$ , respectively. Also, to describe the curvature of the radiating slots in Fig. 1, the following parabolic equation was used [10]:  $x^2/A + x/B + C$ , where  $C = Bi/2$  and the origin was defined at the center of the antenna. The main purpose of the parabolic equation was to assist designers in exactly describing the curvature of the radiating slot. Analytical information such as slot length and slope can be extracted from this equation.

### III. SIMULATION AND MEASUREMENT RESULTS

The prototype antenna in Fig. 3 (top) was designed and simulated in both the commercial software packages ADS [11] and HFSS [12]. Both simulations assumed a 1.4-mm-thick substrate with  $\epsilon_r = 3.55$  and a copper thickness of  $35 \mu\text{m}$ . The prototype antenna was manufactured on a Rogers 4003 [13] substrate that was 1.58 mm thick. The assumed simulation thickness of 1.4 mm compensated for the thickness reduction due to manufacturing. The 50- $\Omega$  CPW transmission line feeding the prototype antenna was designed using AppCAD [14]. Also, the manufactured prototype reported in [7] is shown for size comparison in Fig. 3 (bottom).

#### A. S-Parameters

The results in Fig. 4 show that the dual-band operation of the prototype antenna is apparent at 900 and 2400 MHz. The measurement and simulation results correlate very well, confirming the design of the antenna as well as the two simulation utilities. However, the upper resonance is higher in comparison to simulation results. This is most likely due to tolerances in the manufacturing process.

#### B. Fields

Figs. 5 and 6 display the field plots in the  $yz$ - and  $xz$ -plane at both 900 and 2400 MHz, respectively. Cross polarization is neg-

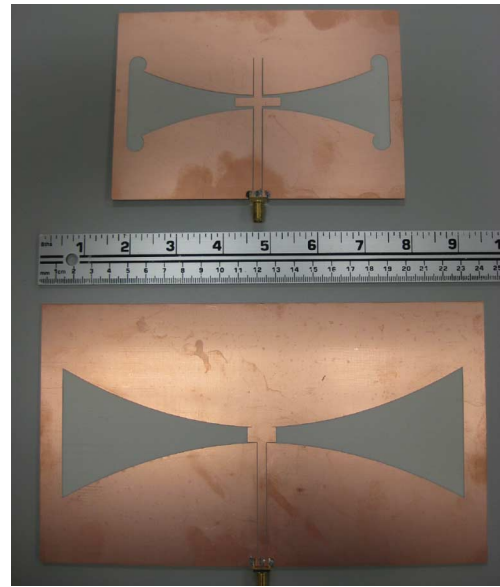


Fig. 3. (top) Compact bow-tie slot antenna produced on Rogers 4003C ( $H = 110$  mm,  $W = 160.0$  mm,  $Bw = 60.2$  mm,  $Bi = 8.0$  mm,  $Bo = 46.1$  mm,  $d = 4.6$  mm,  $g = 0.4$  mm,  $t = 25.0$  mm,  $S = 5.0$  mm,  $S = 5.0$  mm,  $r = 5.0$  mm,  $Bc = 7.3$  mm) compared to (bottom) the bow-tie slot antenna in [7]).

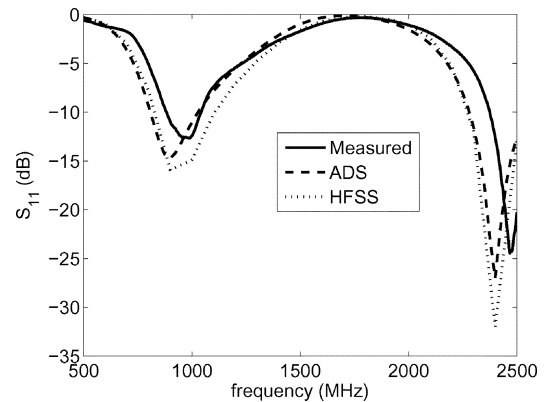


Fig. 4. Simulated and measured  $S_{11}$ .

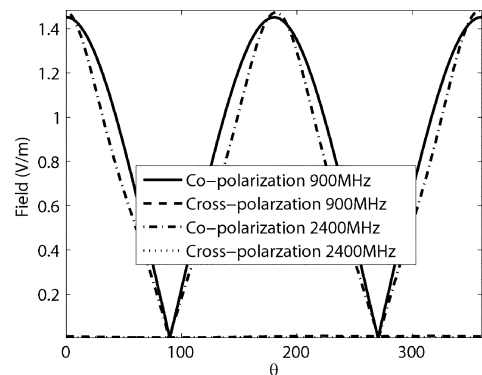


Fig. 5. Field patterns in the  $yz$ -plane simulated in ADS at 900 and 2400 MHz.

ligible in both plots. However, the copolarization at 2400 MHz is slightly higher than the copolarization at 900 MHz.

#### C. Gain

Figs. 7–10 display gain patterns for both the  $yz$ - and  $xz$ -planes at 900 and 2400 MHz. It is shown that the antenna has a max gain of 4.0 dBi at 900 MHz and 6.0 dBi at 2400 MHz.

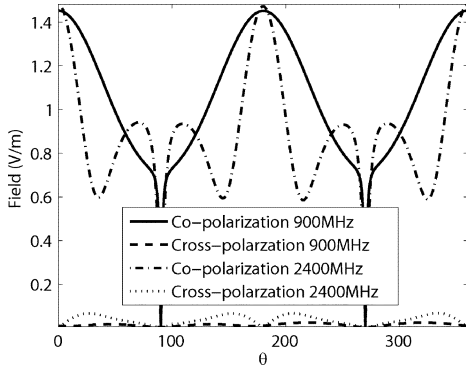


Fig. 6. Field patterns in the  $xz$ -plane simulated in ADS at 900 and 2400 MHz.

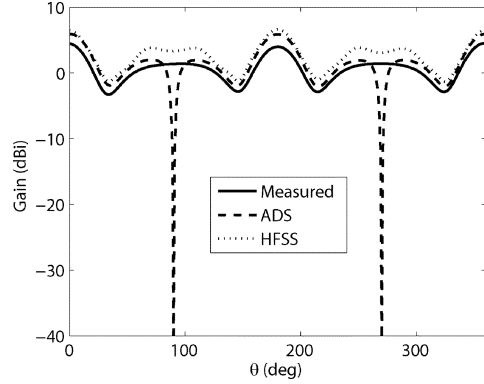


Fig. 10. Simulated and measured gain in the  $xz$ -plane at 2400 MHz.

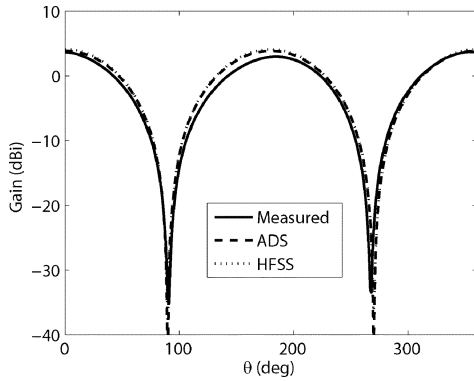


Fig. 7. Simulated and measured gain in the  $yz$ -plane at 900 MHz.

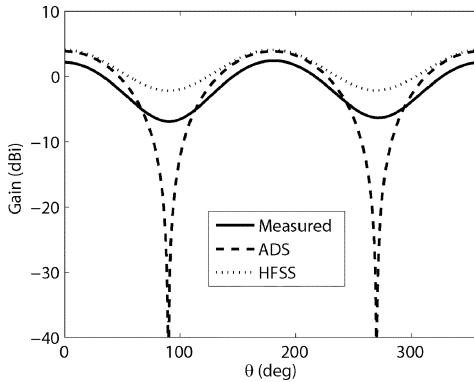


Fig. 8. Simulated and measured gain in the  $xz$ -plane at 900 MHz.

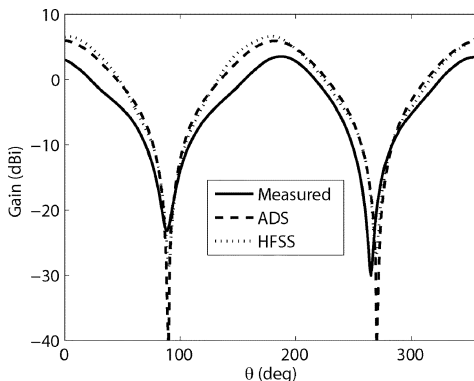


Fig. 9. Simulated and measured gain in the  $yz$ -plane at 2400 MHz.

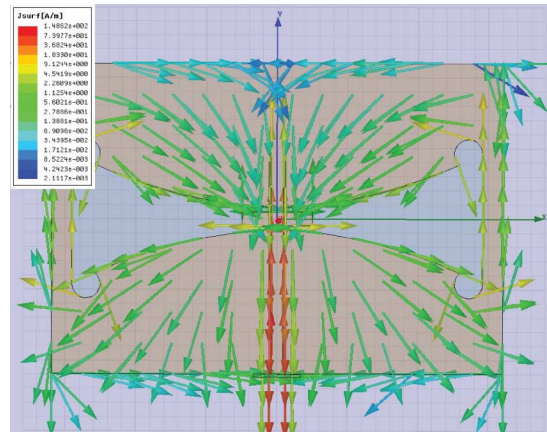


Fig. 11. Surface currents simulated in HFSS at 900 MHz.

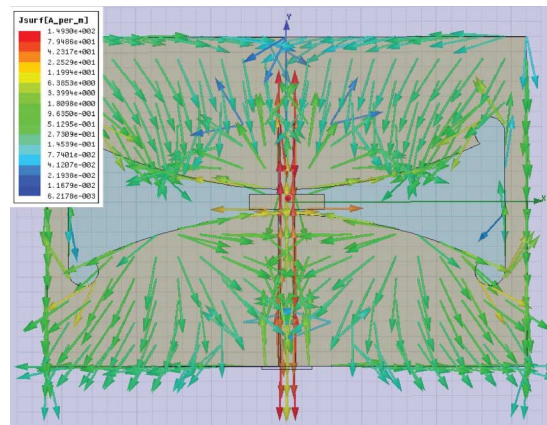


Fig. 12. Surface currents simulated in HFSS at 2400 MHz.

In Figs. 7 and 9, the nulls of the measured gain in the  $xz$ -plane are not as pronounced as the ADS simulation suggests, while the HFSS simulations correlate very well with the measured

results. A possible cause for the difference in simulation results is the infinite substrate layer assumed by ADS and not by HFSS. Additionally, the antenna was measured at a finite distance (near  $10\lambda_1$ ). This may also explain why the measured nulls are not as pronounced as simulation suggests.

#### D. Surface Currents

Fig. 11 displays the surface currents on the antenna at 900 MHz. It is shown that the top slits on the upper half of the antenna force currents traveling toward the center to follow the slit up and then down again, thus increasing the electrical length of the antenna. The surface current plot at 2400 MHz in Fig. 12 displays a similar behavior. The unequal current

TABLE I  
COMPARISON ON THE PERFORMANCE WITH OTHER REPORTED BOW-TIE SLOT ANTENNAS.

Value	[5]	[6]	[7]	[letter]
$f_1$	1.80 GHz	3.50 GHz	900 MHz	900 MHz
Slot width	$0.51\lambda_0$	$0.467\lambda_0$	$0.645\lambda_0$	$0.436\lambda_0$
Slot width	$0.60\lambda_g$	$1.03\lambda_g$	$0.91\lambda_g$	$0.61\lambda_g$
$\epsilon_r$	2.2	10.1	3.55	3.55
h	0.787 mm	1.58 mm	1.40 mm	1.40 mm

dispersion along the slot possibly explains the differences in the  $xz$ -plane gain pattern between 900 and 2400 MHz.

#### IV. DISCUSSION

The goal of the compact bow-tie slot design is to both achieve dual-band operation at 900 and 2400 MHz while reducing the overall size of the antenna. Again,  $\lambda_1$  is the free-space wavelength at 900 MHz and  $\lambda_2$  is the free-space wavelength at 2400 MHz. The dimensions of the slot, CPW stub, and the surrounding ground plane control the operating frequencies of the antenna. For lower band operation, the height  $H$  must be close to  $0.5\lambda_1$ , and the overall width of the slot ( $W - 2Bc$ ) needs to be both approximately  $1.2\lambda_2$  and near  $0.5\lambda_1$ . Furthermore, defining the CPW stub length as  $0.25\lambda_2$  is optimal for upper-band matching. This stub length is similar to the results reported in [15], which presents a folded slot antenna design driven by a CPW transmission line.

Comparing the two designs in Fig. 3, width  $W$  and height  $H$  were reduced from 240 to 160 mm and from 140 to 110 mm, respectively. When compared to the design in [7], this is a decrease of 47% in overall size. However, this size reduction comes at the cost of bandwidth. Further comparison with other published bow-tie slot designs is shown in Table I. The first row shows the lowest operating frequency  $f_1$  for each reported design. The second and third rows show the computed overall slot width of each design using the free-space wavelength  $\lambda_0$  and the guided wavelength  $\lambda_g$ , respectively, of each lowest operating frequency. Finally, for comparison, the fourth and fifth rows show the substrate permittivity and thickness values, respectively. These comparisons show that the antenna presented in this letter has the smallest overall free-space slot width and the second smallest overall substrate guided slot width. The difference when compared to [5] and [7] is quite apparent and demonstrates that significant size reduction can be accomplished without resorting to high dielectric materials such as those used in [6].

The design reported here also improves the gain pattern in the  $yz$ -plane at 2400 MHz. In particular, for this design, the gain at 2400 MHz was 6.0 dBi, which was an increase from the  $-8.17$ -dBi gain reported in [7]. It is believed that this increase in gain is due to the length of the parabolic radiating slot. The overall length of the radiating slot presented in this letter was approximately  $1.2\lambda_2$ , and the overall length of the radiating slot for the design reported in [7] was approximately  $1.5\lambda_2$ . The radiation pattern of the antenna with the  $1.2\lambda_2$ -wide radiating slot has a single main radiation lobe with very low sidelobes (this can be observed in Figs. 9 and 10), where the radiation pattern of the antenna with the  $1.5\lambda_2$  wide radiating slot has multiple sidelobes that are larger than the main lobe. These sidelobes of the  $1.5\lambda_2$  radiation slot reduce the gain of

the antenna reported in [7]. This gain reduction and increased sidelobe behavior is consistent with previously reported electrically long dipole antennas [16]. Finally, the gain at 900 MHz exhibits a small decrease from 4.62 dBi in [7] to 4.0 dBi in the  $yz$ -plane. The field plots also reiterate this observation and are comparable to the values reported in [15].

The addition of the top slits in this design improves the overall impedance match and the radiation pattern characteristics of the antenna. This makes the design presented in this letter more desirable when compared to the antenna reported in [7].

#### V. CONCLUSION

In this letter, two methods to reduce the overall size of a dual-band bow-tie slot antenna are presented. In particular, techniques for extending the coplanar waveguide feeding the antenna and sweeping the radiating slots in a circular manner are presented. It is shown that by combining these two techniques to design a single dual-band (900 and 2400 MHz) bow-tie slot antenna, the overall size can be reduced by as much as 47%. In addition to the size reduction benefits, the gain is increased at 2400 MHz when compared to a similar but larger antenna. Throughout this letter, simulations from two different commercially available simulation tools are shown to compare very well with measurements. The addition of top slits and modifying the radiating slots in a circularly swept manner gives the design in this letter benefits over other reported designs in literature in the form of smaller size and lower frequencies of operation.

#### REFERENCES

- [1] Y.-D. Lin and S.-N. Tsai, "Coplanar waveguide-fed uniplanar bow-tie antenna," *IEEE Trans. Antennas Propag.*, vol. 45, no. 2, pp. 305–306, Feb. 1997.
- [2] E. Soliman, S. Brebels, P. Delmotte, G. Vandenbosch, and E. Beyne, "Bow-tie slot antenna fed by CPW," *Electron. Lett.*, vol. 35, no. 7, pp. 514–515, Apr. 1999.
- [3] Y. Chen, C. Ruan, and L. Peng, "A novel ultra-wideband bow-tie slot antenna in wireless communication systems," *Prog. Electromagn. Res. Lett.*, vol. 1, pp. 101–108, 2008.
- [4] S.-H. Wi, J.-M. Kim, T.-H. Yoo, H.-J. Lee, J.-Y. Park, J.-G. Yook, and H.-K. Park, "Bow-tie-shaped meander slot antenna for 5 GHz applications," in *IEEE AP-S/URSI Symp. Dig.*, 2002, vol. 2, pp. 456–459.
- [5] L. Marantis and P. Brennan, "A CPW-fed bow-tie slot antenna with tuning stub," in *Proc. Loughborough Antennas Propag. Conf.*, Loughborough, U.K., 2008, pp. 389–392.
- [6] M. Miao, B. Ooi, and P. Kooi, "Broadband CPW-fed wide slot antenna," *Microw. Opt. Technol. Lett.*, vol. 25, no. 3, pp. 206–211, 2000.
- [7] L. A. Berge, M. T. Reich, M. A. Aziz, and B. D. Braaten, "Tuning a bow-tie slot antenna with an equation based curve for 900 MHz and 2400 MHz ISM bands," Dept. Elect. Comput. Eng., North Dakota State Univ., Fargo, ND, Tech. Rep., 2011 [Online]. Available: <http://hdl.handle.net/10365/18312>
- [8] J. Mandeep and M. Nicholas, "Design an X-band Vivaldi antenna," *Microw. RF*, vol. 47, no. 8, 2008.
- [9] R. Waterhouse, *Printed Antennas for Wireless Communications*. Hoboken, NJ: Wiley, 2007, p. 234.
- [10] E. Kreyszig, *Advanced Engineering Mathematics*, 8th ed. Hoboken, NJ: Wiley, 1999, p. 234.
- [11] Advanced Design System. Agilent Technologies, Santa Clara, CA, 2009.
- [12] High Frequency Structure Simulator. ver. 12.1, Ansys Inc., Canonsburg, PA, 2010.
- [13] "Rogers Corporation," Rogers Corporation, Rogers, CT [Online]. Available: <http://www.rogerscorp.com>
- [14] AppCAD. Agilent Technologies, Santa Clara, CA, 2002.
- [15] D. E. Anagnostou and A. A. Gheethan, "A coplanar reconfigurable folded slot antenna without bias network for WLAN applications," *IEEE Antennas Wireless Propag. Lett.*, vol. 8, pp. 1057–1060, 2009.
- [16] W. L. Stutzman and G. A. Thiele, *Antenna Theory and Design*, 2nd ed. New York: Wiley, 1998.